

## Surface profiling by frequency-domain analysis of white light interferograms

Peter de Groot and Leslie Deck

Zygo Corporation, Laurel Brook Road, Middlefield, CT 06455

Three-dimensional imaging interferometric microscopes have outstanding accuracy, provided of course that the test objects are sufficiently smooth and continuous. The present study shows that a white-light source and spatial-frequency domain analysis of the resulting interferograms can dramatically increase the range of application of interferometric surface profilers.<sup>1,2</sup> This analysis breaks the white light up into its constituent colors and makes it possible to apply multiple-wavelength techniques to the problem of surface height measurement.

In an ideal dispersion-corrected interferometer with a monochromatic source, the interferometric phase  $\theta$  is related to the round-trip optical path difference  $x$  by

$$\theta = kx, \quad (1.)$$

where  $k = 2\pi/\lambda$  is the angular wavenumber of the source light. As a consequence, there is a simple relationship between the rate of change of phase with wavenumber and the path length:

$$d\theta/dk = x. \quad (2.)$$

Measuring distances with the aid of Eq.(2.) has some distinct advantages when compared to conventional phase-shifting interferometry,<sup>3</sup> the most outstanding of which is the reduction or elimination of any embarrassment resulting from  $2\pi$  phase ambiguities. This makes it possible to use interferometry with surfaces that are rough or discontinuous on the scale of an optical wavelength.

The fact that distances can be measured by observing how the interferometric phase changes as a function of wavenumber has given rise to a wide variety of instruments variously described as wavelength-shift interferometers, chirp laser radars, coherence radars, peak-fringe scanning microscopes, laser multiwavelength interferometers, synthetic wavelength laser gages, low-coherence interferometers, coherence scanning microscopes, absolute-distance interferometers and so on, depending on the particular implementation of the principle. All of these instruments and methods use some equivalent form of Eq.(2.) and the rate of change of phase with wavelength to measure path lengths. It is easy to get lost in the details of how this rate of change is determined, particularly with white-light and low-coherence methods, which for the most part don't involve any direct calculation of phase angles. However, recognizing that the same basic principle is involved can be very useful in the selection of a data processing scheme.

In white light interferometry the point of highest fringe contrast -- the coherence peak -- is the most distinctive feature of the broadband interferogram. Most optical profilers based on white light process the interference data in order to determine the position of the coherence peak.<sup>4</sup> These profilers differ mostly in the way they detect and process the fringe-contrast envelope. Balasubramanian oscillates a reference mirror with a PZT to calculate the fringe contrast, and then repeats the calculation for a succession of points in space in order to trace out the contrast envelope.<sup>5</sup> Caber has developed more flexible and accurate formulas for calculating the fringe contrast, and also with more powerful methods of estimating the fringe contrast peak with sparse data using curve fitting.<sup>6</sup> Kino and Chim transform their data to the spatial-frequency domain, eliminate the negative frequencies, center the positive frequency packet around zero and then transform back to the original data domain to reveal a carrier-suppressed envelope for further processing.<sup>7</sup> Fercher et al.<sup>8</sup> have dynamic data acquisition for one-dimensional scans using an analog band-pass filter and storage of a signal strength that is proportional to the fringe contrast.

How does these fringe-contrast envelope methods relate to the rate of change of interferometric phase with wavenumber? In the absence of chromatic dispersion, the coherence peak corresponds to the position at which the rate of change of phase  $d\theta/dk$  is equal to zero. Thus the best fringe contrast occurs at the so-called stationary phase point.<sup>9</sup> This makes intuitive sense: If the phase isn't changing with wavelength, then all the different wavelengths are in phase and contribute constructively to the interference pattern. Thus all of the methods that dissect the fringe-contrast envelope are based on a search for the exact position of stationary phase. However, as Eq.(2.) shows, the distance to the stationary phase point is easy to calculated once  $d\theta/dk$  is known at any given position in the interferogram. Thus it is not really necessary to detect

the contrast envelope and extrapolate to the peak in order to measure distances or surface features unambiguously with white light.

Now let's take a look at some hardware. Figure 1 shows the optical configuration of a scanning white-light interferometric microscope. Interferograms for a each of the image points in the field of view of the instrument are generated simultaneously by scanning the object in a direction perpendicular to the object surface, while recording detector data in digital memory. For some objects of interest, a scan length of several tens of microns is required to accommodate all of the surface features. We use a simple frequency-based discriminator sensitive to variations in the data to determine when to store data for each pixel.<sup>10</sup> In this way, the total number of points stored and processed remains fixed for all scan lengths.

To calculate the rate of change of phase  $d\theta/dk$  for a particular image pixel, we need the individual interferometric phases corresponding to a few of the constituent wavenumbers of the source, so that we can see what the trend is. The only real problem is how to isolate phases for individual wavelengths when the information is all mashed together into one white-light interferogram. The problem is solved by performing a digital Fourier Transform of the interferogram, which now is represented by its complex frequency-domain spectrum, made up of amplitudes and phases as a function of spatial frequency.

Once the interference data has been transformed into the frequency domain, we select a series of pairs  $(\theta_j, k_j)$ , do a least-squares linear fit to find the ratio, and obtain  $d\theta/dk$ . As an added bonus, the intercept of the least-squares fit can be used to generate an excellent estimate of the interferometric phase for the mean wavenumber. The mean phase value together with the rate of change of phase with wavenumber can be combined to calculate surface heights with the same accuracy as conventional phase-shifting interferometry without  $2\pi$  phase ambiguities. The frequency-domain calculations are repeated for every pixel in the field of view to generate a complete, three-dimensional image of the surface. In our experiments, we typically achieve an RMS repeatability of 0.5nm for successive measurements of smooth, flat surfaces.

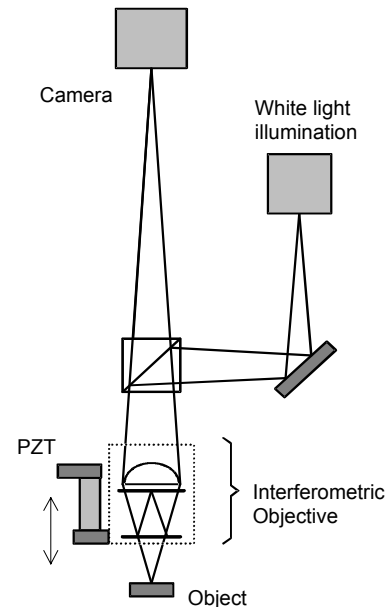


**Figure 1:** The scanning white-light interferometer.

Examples of three-dimensional images obtained by frequency-domain processing of white-light fringes are presented Figure 2. These plots demonstrate that the interferometer has a large unambiguous range, and is capable of profiling surfaces generally not considered appropriate for interferometry. This capability, coupled with the high accuracy of the technique, makes white-light frequency-domain processing an attractive method of surface profiling.

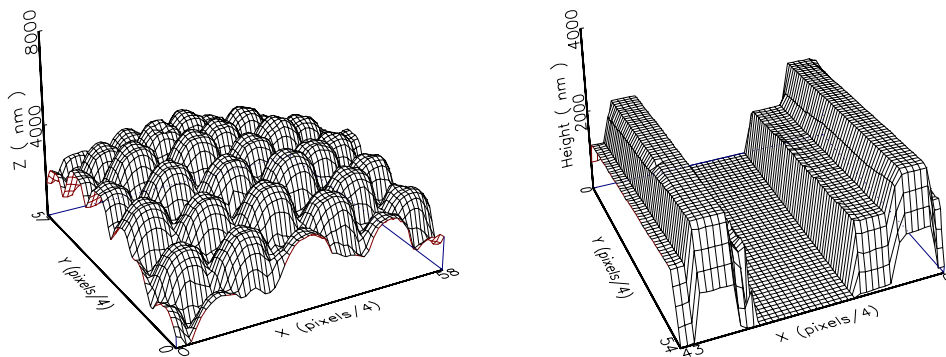


**Figure 2:** Results of surface topography measurements. The left-hand plot shows a moth's eye, and the right-hand plot shows the profile of a sensing head for a magnetic-storage hard disk drive.

## References

- <sup>1</sup> P. de Groot and L. Deck, *Opt. Lett.* **18**(17), 1462-1464 (1993).
- <sup>2</sup> P. de Groot and L. Deck, *J. Mod. Opt.* (to appear).
- <sup>3</sup> J. E. Greivenkamp and J. H. Bruning, in *Optical Shop Testing*, Daniel Malacara, Ed. (Wiley, New York, 1992), Chap. 14.
- <sup>4</sup> J. C. Wyant, *Laser Focus World* (September), 131-135 (1993).
- <sup>5</sup> N. Balasubramanian, U.S. Patent #4,340,306 (Jul. 20, 1982).
- <sup>6</sup> P. J. Caber, *Appl. Opt.* **32**(19), 3438-3441 (1993).
- <sup>7</sup> Gordon S. Kino and Stanley S.C. Chim, *Appl. Opt.* **29**(26), 3775-3783 (1990).
- <sup>8</sup> A.F. Fercher, K.Mengedocht and W. Werner, *Opt. Lett.* **13**(3), 186-188 (1988).
- <sup>9</sup> B.L. Danielson and C.Y. Boisrobert, *Appl. Opt.* **30**(21), 2975-2979 (1991).
- <sup>10</sup> L. Deck and P. de Groot, *Proc. ASPE* 424-426 (1993).